

Structural Heterogeneity of Ag^I Complexes with a Flexible 1,2-Bis[(imidazol-2-yl)thiomethyl]benzene Ligand and Issues Regarding the Phase Purity of the Bulk Material

Liliana Dobrzańska*^[a,b]

Keywords: Silver / Ligand flexibility / Coordination modes / Phase purity / X-ray diffraction

A series of Ag^I coordination compounds with a new ligand, 1,2-bis[(imidazol-2-yl)thiomethyl]benzene, and counterions such as PF₆⁻, SbF₆⁻, CF₃SO₃⁻, BF₄⁻ and NO₃⁻ was characterised by powder and single-crystal XRD. Powder XRD revealed the presence of a mixture of crystallographic phases that were further identified by single-crystal XRD. Despite conformational flexibility, 1,2-bis[(imidazol-2-yl)thiomethyl]benzene has a tendency to form *N,N*-chelated Ag^I mononuclear cationic complexes with a linear N–Ag^I–N unit. However, T-shaped geometry (N₂O) around the silver ion was also observed, which involved solvent molecules and/or counterions. The formation of a cationic 1D chain with the *N,N'*-bridging ligand was revealed with the BF₄⁻ counterion. Coordination

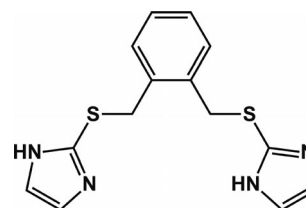
compounds that possess different nuclearity were formed with the NO₃⁻ counterion. In the dinuclear and trinuclear complexes, the ligand showed bischelating behaviour with N-donor atoms that interact with one and S-donor atoms with another metal centre. Furthermore, the crystal structure of the trinuclear complex revealed the presence of two crystallographically independent cationic moieties in the asymmetric unit, which only differ by a single O-donor ligand (NO₃⁻ vs. H₂O), where both of the moieties possess three different geometries around the constituent silver ions. Argentophilic interactions are present in the majority of the reported structures. Available amine N atoms facilitate hydrogen bond formation and promote the occurrence of solvates.

Introduction

During the last three decades, coordination chemistry has increasingly been involved with more elaborate ligands and studies of metal–organic complexes with extended structures of different topologies.^[1] This led to the discovery of new, interesting properties connected with porosity, chirality, magnetism and nonlinear optics, as well as the emergence of related applications for these materials.^[2] Imidazole-based ligands have been investigated for many years. Initially, complexes with simple imidazole rings were studied with focus on detailed spectroscopic and structural characteristics.^[3] When interest shifted to more complicated linkers, the incorporation of imidazole rings was justified by their reputation as effective N-donor building blocks.^[4]

In continuation of our studies on imidazole-based extended linkers,^[5] an investigation of the coordination chemistry of Ag^I complexes with a new ligand, 1,2-bis[(imidazol-2-yl)thiomethyl]benzene (**L**, Scheme 1), was undertaken.^[6] **L** is more flexible than ligands that we have previously studied due to the presence of a thioether linkage.^[7] How-

ever, the *ortho*-position of the thioimidazole substituents on the benzene ring provides some rigidity in **L**. Previously reported Ag^I complexes with a similar ligand, 1,2-bis(2-methylimidazol-1-ylmethyl)benzene (with 2-methylimidazole rings in the *ortho*-position), revealed the formation of 1D chains with PF₆⁻, SbF₆⁻ and BF₄⁻ counterions in a metal/ligand ratio of 1:1 as the 2-methyl groups successfully prevent the formation of mononuclear species.^[8] As will be discussed further, elongation of the linker by the incorporation of an S-donor atom and, even more importantly, the presence of a free NH in the imidazole ring, make the prediction of the final products more complicated.



Scheme 1. 1,2-Bis[(imidazol-2-yl)thiomethyl]benzene (**L**).

[a] Department of Chemistry, Katholieke Universiteit Leuven, Celestijnenlaan 200F, 3001 Heverlee, Belgium
Fax: +32-16-327-990
E-mail: lianger@chem.kuleuven.be

[b] Department of Chemistry and Polymer Science, Stellenbosch University,
Private Bag X1, Matieland 7602, South Africa

Supporting information for this article is available on the WWW under <http://dx.doi.org/10.1002/ejic.201100853>

Results and Discussion

All metal complexes were prepared similarly in a dark environment with an Ag/**L** ratio of 1:1 (0.2:0.2 mmol). A solution of silver salt (AgPF₆ for **1**, AgSbF₆ for **2**,

AgCF₃SO₃ for **3**, AgBF₄ for **4** and AgNO₃ for **5** in MeOH (15 mL) was added to a solution of **L** in MeOH (25 mL). The mixture was stirred for a few minutes and the resulting clear solution was left to stand for ca. four weeks until crystalline material formed. Single crystals of **1–5** were isolated from each vial and XRD measurements were performed to reveal the presence of [AgL]PF₆·CH₃OH (**1a**) in **1**, [AgL]SbF₆ (**2a**) in **2**, [AgL]CF₃SO₃·H₂O (**3a**) in **3**, {[AgL]BF₄}_n (**4a**) in **4** and [Ag₂L(NO₃)₂] (**5a**) in **5**.

Powder XRD Studies

Powder XRD (XRPD) analyses were performed to assess the purity of the phases obtained.^[9a] As there was no agreement between the powder patterns generated from the single-crystal structures (labelled as **a**) and the measured powder patterns of the corresponding bulk material (Supporting Information, Figures S1–S5),^[9b] a further study was performed to identify the remaining crystallographic phases. This way, new crystal structures were revealed (Table S1). PowderCell 2.4 freeware was used to further estimate the percentage of the respective crystallographic phases (Figures S6–S9).^[9c] It is not certain that all the phases were identified, but the results seem to indicate that at the time of the XRPD measurement, the respective compositions were as follows. Complex **1b**, which contains water molecules in the crystal lattice, was the major component of **1** (more than 50%). Complex **2b**, which also contains water molecules, was the dominant phase in **2** (over 80%). In **4**, mononuclear **4b** was the major constituent (ca. 80%) over polynuclear complex **4a**. Complexes **5c** and **5a**, which show bischelating behaviour and have coordinated nitrate ions, were the preferred phases in **5**, and the presence of mononuclear, cationic **5b** was negligible.

Single-Crystal XRD Studies

Crystal Structures of **1a**, **1b**, **1c** and **1d** Formed with PF₆[−] (Bulk Material **1**)

[AgL]PF₆·CH₃OH (**1a**)

Complex **1a** crystallises in the monoclinic space group *P*2₁/*c* and contains one mononuclear cationic Ag^I complex, one PF₆[−] counterion and one molecule of methanol in the asymmetric unit (Figure 1). The silver atom in the complex is linearly coordinated by the two imine N atoms that originate from the chelating imidazole rings of the ligand (for bond lengths, see Table 2). The ligand adopts a folded conformation (Table 3) with a dihedral angle of ca. 34° between the planes of the imidazole rings and the benzene ring. The methanol molecule interacts with the amine N atom of the cationic unit and the counterion by hydrogen bonding.

The solvent molecule acts as a hydrogen bond acceptor and donor simultaneously (Table S2). The distance between neighbouring Ag ions indicates the presence of very weak interactions between the Ag centres from nearby mononuclear units (this conclusion was drawn by comparison with

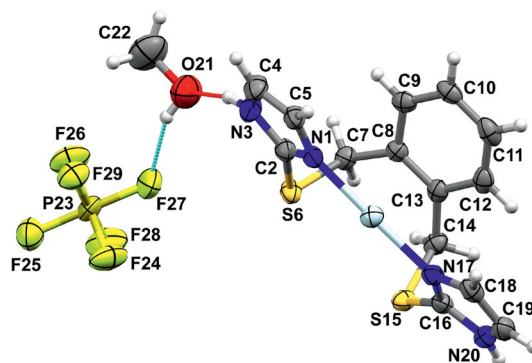


Figure 1. Asymmetric unit of **1a** with displacement ellipsoids drawn at the 50% probability level and hydrogen bonding shown in red and blue.

the results below; see also Table 4)^[10] supported by weak interactions between imidazole rings from corresponding mononuclear complexes with a centroid–centroid distance of 3.507(2) Å (symmetry operation: $-x, 1 - y, -z$). Looking down the *b* axis, columns of dimeric cationic complexes stacked above each other are observed. These interact further by C5–H5⋯S6^{#4} interactions [C5⋯S6 3.396(4) Å, for symmetry operations, see Table S2]. The dimeric units expand along the *c* axis and are further held together by C–H⋯π interactions between C10–H10⋯Cg1^{#6} [where Cg1 is the centroid of the benzene ring belonging to the dimeric unit from a neighbouring column; C10⋯Cg1 3.545(4) Å] to form layers. These layers are separated by rows of alternating pairs of solvent molecules and counterions (Figure 2). Weak N–H⋯F and C–H⋯F interactions support the packing (Table S2).

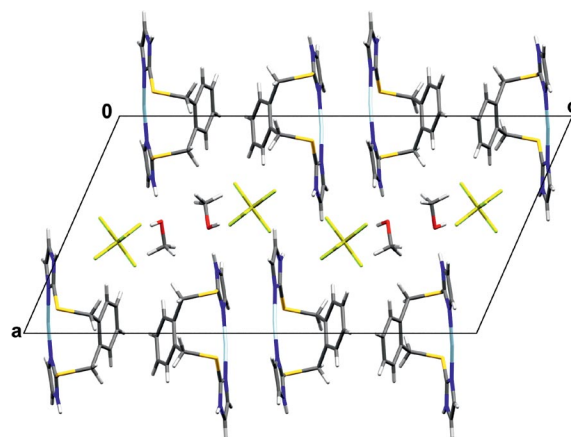


Figure 2. Representation of the packing of **1a** viewed down the *b* axis.

[AgL]PF₆·H₂O (**1b**)

The unit cell parameters of the crystal structure of **1b** are very similar to those of **1a**, as are the main structural features of the compound (the same type of coordination sphere around the metal atom in the monomeric cationic complex). A water molecule takes more or less the same space that was previously occupied by the methanol mole-

cule but it is badly disordered and modelled in four positions. An interaction between the water molecule and the counterions is suspected but is not confirmed due to the disorder present. The smaller size of solvent molecules causes the neighbouring mononuclear cationic complexes to pack closer, which shortens the distance between the silver ions (Table 4). This is also noticeable by a minor decrease of the length of the *c* axis (Table 1). Negligible changes can also be seen in the position of the counterions. The water molecule shows interactions with the amine N atom. It might also interact with the counterions, but the disorder present renders it impossible to make any further assumptions.

[AgL]PF₆·xCH₃OH·xH₂O (1c)

Complex **1c** crystallises in the monoclinic space group *C2/c* with unit cell parameters different from those of **1a/1b** but very close to those obtained for **2b** (Table S1). Unfortunately, the quality of the crystals was too poor to fully characterise the compound.

[AgLCH₃O(H)_{0.5}](PF₆)_{0.5} (1d)

Complex **1d** crystallises in the same monoclinic space group *P2₁/c* as **1a** and **1b**, but the unit cell parameters, the conformation of the ligand and the packing are completely different. It consists of one mononuclear cationic unit, $[AgLCH_3O(H)_{0.5}]$, and half a PF₆[−] ion (the P atom is lo-

Table 1. Crystal data and details of the refinement parameters for the crystal structures originating from crystalline bulk material 1–5.

	1a	1b	1d	2a	2b
Formula	C ₁₅ H ₁₈ AgF ₆ N ₄ OPS ₂	C ₁₄ H ₁₆ AgF ₆ N ₄ OPS ₂	C ₃₀ H ₃₅ Ag ₂ F ₆ N ₈ O ₂ PS ₄	C ₁₄ H ₁₄ AgF ₆ N ₄ S ₂ Sb	C ₂₈ H ₃₄ Ag ₂ F ₁₂ N ₈ O ₃ S ₄ Sb ₂
Formula weight	587.29	573.27	1028.61	646.03	1346.11
Crystal system	monoclinic	monoclinic	monoclinic	triclinic	monoclinic
Space group	<i>P2₁/c</i>	<i>P2₁/c</i>	<i>P2₁/c</i>	<i>P</i> $\bar{1}$	<i>C2/c</i>
<i>T</i> [K]	100(2)	100(2)	100(2)	100(2)	100(2)
λ [Å]	0.71073	0.71073	0.71073	0.71073	0.71073
<i>a</i> [Å]	12.9254(13)	12.9855(15)	11.1343(14)	8.7694(11)	28.540(2)
<i>b</i> [Å]	7.1323(7)	7.0940(8)	20.194(3)	10.5672(14)	7.0078(6)
<i>c</i> [Å]	24.719(3)	24.637(3)	8.5647(11)	11.6747(15)	24.697(2)
α [°]	90	90	90	73.364(2)	90
β [°]	113.873(2)	115.260(2)	105.204(2)	70.131(2)	120.7380(10)
γ [°]	90	90	90	80.474(2)	90
<i>V</i> [Å ³]	2083.8(4)	2052.5(4)	1858.3(4)	972.1(2)	4245.6(6)
<i>Z</i>	4	4	2	2	4
<i>D</i> _{calc} [g cm ^{−3}]	1.872	1.855	1.838	2.207	2.106
μ Mo- <i>K</i> α [mm ^{−1}]	1.313	1.330	1.394	2.675	2.459
Crystal size [mm]	0.31 × 0.27 × 0.23	0.27 × 0.17 × 0.13	0.17 × 0.13 × 0.04	0.32 × 0.27 × 0.19	0.31 × 0.28 × 0.20
Unique reflections (<i>R</i> _{int})	4960 (0.0390)	4877(0.0514)	3862 (0.0639)	4419 (0.0185)	4995 (0.0390)
Reflections with <i>I</i> > 2 σ (<i>I</i>)	4699	4007	2998	4194	3965
Refined parameters	275	295	243	253	313
<i>R</i> ₁ ^[a] , <i>wR</i> ₂ ^[b] [<i>I</i> > 2 σ (<i>I</i>)]	0.0470, 0.1236	0.0719, 0.1746	0.0639, 0.1485	0.0228, 0.0544	0.0367, 0.0768
<i>R</i> ₁ ^[a] , <i>wR</i> ₂ ^[b] (all data)	0.0488, 0.1250	0.0892, 0.1834	0.0840, 0.01584	0.0247, 0.0554	0.0525, 0.0829
Goodness-of-fit on <i>F</i> ²	1.099	1.098	1.050	1.075	1.001
	3a	4a	5a	5b	5c
Formula	C ₁₅ H ₁₆ AgF ₃ N ₄ O ₄ S ₃	C ₁₄ H ₁₄ N ₄ S ₂ Ag·BF ₄	C ₁₄ H ₁₄ Ag ₂ N ₆ O ₆ S ₂	C ₁₄ H ₁₄ N ₄ S ₂ AgNO ₃ ·xH ₂ O	C ₅₆ H ₆₆ Ag ₆ N ₂₂ O ₂₃ S ₈
Formula weight	577.40	497.09	642.17	472.29	2319.01
Crystal system	triclinic	triclinic	triclinic	triclinic	triclinic
Space group	<i>P</i> $\bar{1}$	<i>P</i> $\bar{1}$	<i>P</i> $\bar{1}$	<i>P</i> $\bar{1}$	<i>P</i> $\bar{1}$
<i>T</i> [K]	100(2)	100(2)	100(2)	100(2)	100(2)
λ [Å]	0.71073	0.71073	0.71073	0.71073	0.71073
<i>a</i> [Å]	9.5218(13)	7.1716(19)	8.0267(8)	9.5430(6)	8.1077(4)
<i>b</i> [Å]	10.1352(14)	11.525(3)	9.8371(10)	11.6976(8)	20.6967(12)
<i>c</i> [Å]	11.6408(16)	12.239(3)	13.6870(14)	17.2051(11)	24.0920(13)
α [°]	72.271(2)	107.444(4)	102.580(2)	84.1350(10)	94.4590(10)
β [°]	74.598(2)	101.474(4)	102.482(2)	82.6390(10)	90.1730(10)
γ [°]	82.707(2)	107.357(4)	105.798(2)	79.7250(10)	98.8550(10)
<i>V</i> [Å ³]	1030.3(2)	873.7(4)	970.30(17)	1868.0(2)	3982.0(4)
<i>Z</i>	2	2	2	4	2
<i>D</i> _{calc} [g cm ^{−3}]	1.861	1.889	2.198	1.679	1.934
μ Mo- <i>K</i> α [mm ^{−1}]	1.340	1.439	2.281	1.325	1.742
Crystal size [mm]	0.34 × 0.19 × 0.17	0.24 × 0.21 × 0.03	0.18 × 0.09 × 0.02	0.23 × 0.11 × 0.03	0.34 × 0.27 × 0.07
Unique reflections (<i>R</i> _{int})	4776 (0.0366)	4024 (0.0628)	4451 (0.0333)	8565 (0.0298)	14825 (0.0513)
Reflections with <i>I</i> > 2 σ (<i>I</i>)	4148	3270	3806	7843	11831
Refined parameters	271	235	271	451	1106
<i>R</i> ₁ ^[a] , <i>wR</i> ₂ ^[b] [<i>I</i> > 2 σ (<i>I</i>)]	0.0415, 0.0915	0.0806, 0.1957	0.0477, 0.1102	0.0583, 0.1367	0.0448, 0.0888
<i>R</i> ₁ ^[a] , <i>wR</i> ₂ ^[b] (all data)	0.0501, 0.0958	0.1013, 0.2079	0.0594, 0.1163	0.0646, 0.1398	0.0612, 0.0945
Goodness-of-fit on <i>F</i> ²	1.040	1.048	1.047	1.167	1.031

[a] $R_1 = \sum ||F_o| - |F_c|| / \sum |F_o|$. [b] $wR_2 = \{ \sum [w(F_o^2 - F_c^2)^2] / \sum [w(F_o^2)^2] \}^{1/2}$.

cated on an inversion centre). The methanol molecule is coordinated to the metal centre and, to balance the charge, is partially deprotonated. The cationic complex in this compound is triangular as the result of the conformation adopted by the ligand, with one of the thioether bridges pointing above and the other below the plane of the benzene ring and the imidazole rings tilted towards each other with a dihedral angle between their planes of $42.8(2)^\circ$ (Figure 3).

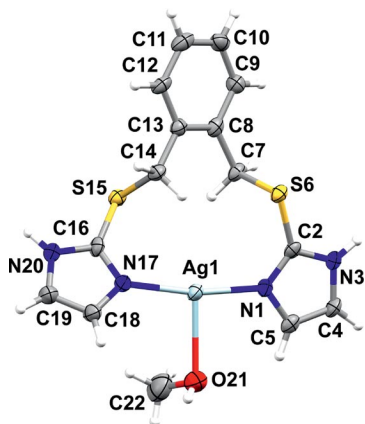


Figure 3. Representation of the cationic complex in **1d** with displacement ellipsoids drawn at the 50% probability level.

The coordinated methanol molecule [Ag1–O21 2.568(6) Å] together with the imine N atoms from the chelating ligand form a T-shaped geometry around the Ag ion. There are no argentophilic interactions present. The amine N atom interacts with the counterions that are additionally involved in interactions with the methanol molecules (Table S2). Hydrogen bonding of the latter probably causes the distortion from linearity of the N–Ag–N unit with an angle of $167.9(2)^\circ$. Furthermore, π – π interactions are present between neighbouring N1–C5 imidazole rings as well as C–H \cdots π interactions between C12–H12 \cdots Cg2^{#6} [where Cg2 is the centroid of the N1–C5 imidazole ring with a C \cdots Cg2 distance of 3.324(6) Å] and C4–H4 \cdots S15^{#5} contacts [C \cdots S 3.774(6) Å], which support the packing.

Crystal Structures of **2a** and **2b** Formed with SbF_6^- (Bulk Material 2)

$[\text{AgL}]\text{SbF}_6$ (**2a**)

Complex **2a** crystallises in the triclinic space group $P\bar{1}$, with one cationic $[\text{AgL}]^+$ complex and one SbF_6^- counter-

ion in the asymmetric unit. There are no solvent molecules present. The silver ion is linearly coordinated by the two N atoms that originate from the imidazole rings of the chelating ligand (for bond lengths, see Table 2), and the ligand has a folded conformation with both thioether bridges on the same side of the plane of the benzene ring (Table 3). The values of the two C–C–S–C torsion angles are disproportionate, which causes the benzene ring to tilt to one side. Argentophilic interactions are present (Table 4) and form a dimeric species supported by π – π interactions between neighbouring imidazole rings with a distance of 3.632(2) Å between the corresponding centroids.

In the packing motif, cationic silver complexes linked in dimers are stacked above each other (as in **1a** and **1b**) with benzene rings from neighbouring columns in the same row pointing in opposite directions (as they are related by an inversion centre, Figure 4). The rows are separated by counterions. N–H \cdots F and C–H \cdots F hydrogen bonds support the close packing (Table S2).

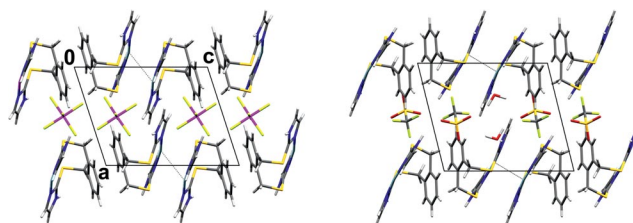


Figure 4. Representation of the packing viewed down the *b* axis for **2a** (left) and **3a** (right); argentophilic interactions are shown as dashed grey lines.

$[\text{AgL}]\text{SbF}_6 \cdot 1.5\text{H}_2\text{O}$ (**2b**)

Complex **2b** crystallises in the monoclinic space group $C2/c$. There is one mononuclear cationic silver complex, one counterion and 1.5 water molecules in the asymmetric unit. The silver ion is linearly coordinated by two imine N atoms from the chelating ligand (see Table 2), and the ligand adopts a folded conformation (see Table 3).

The cationic complex forms dimers that are held together by argentophilic interactions, which are supported by weak interactions between opposite imidazole rings with a centroid–centroid distance of 3.653(3) Å (symmetry operation: $1/2 - x, 1/2 - y, -z$). Looking down the *b* axis, the packing of the cationic complexes resembles that of **1a/1b**, i.e. with the formation of rows that consist of dimeric units with benzene rings from neighbouring columns pointing in the same direction. This enables C–H \cdots π interactions, namely, C11–H11 \cdots Cg1^{#7} (where Cg1 is the centroid of

Table 2. Selected bond lengths [Å] and angles [°] for mononuclear **1–5**.

	1a	1b	1d	2a	2b	3a	5b
Ag1–N1	2.088(3)	2.090(6)	2.113(5)	2.108(2)	2.095(3)	2.109(3)	2.133(5)/2.132(5)
Ag1–N17	2.085(3)	2.092(6)	2.133(5)	2.125(2)	2.097(3)	2.107(3)	2.134(4)/2.137(4)
Ag2–O21			2.568(6)				
N17–Ag1–1	173.39(11)	171.9(2)	167.9(2)	170.63(7)	171.74(12)	172.28(11)	163.66(17)/163.39(1)
N1–Ag1–O21			89.20(18)				
N17–Ag1–O21			99.77(19)				

Table 3. Torsion angles [°] that show the flexibility of the ligand in the Ag^I complexes, for corresponding values in **5c**, see main text.

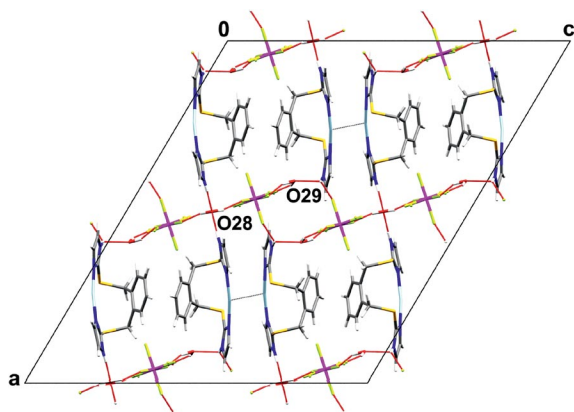
	C8–C7–S6–C2	C13–C14–S15–C16
1a	55.3(3)	–56.6(3)
1b	56.3(6)	–54.2(6)
1d	170.3(4)	–177.6(4)
2a	41.3(2)	–68.6(2)
2b	52.9(4)	–58.6(3)
3a	59.8(3)	–55.3(3)
4a	71.9(7)	–175.0(6)
5a	49.7(4)	–51.0(4)
5b	63.9(5)/64.4(5)	–60.8(6)/–57.1(5)

Table 4. Argentophilic interactions.^[10]

	Silver–silver interaction [Å]
1a	3.4459(6) intermolecular
1b	3.3621(9) intermolecular
1d	–
2a	3.2378(5) intermolecular
2b	3.3418(6) intermolecular
3a	3.2845(6) intermolecular
4a	3.4474(14) intermolecular
5a	2.9558(6) intramolecular
5b	–
5c	3.0919(5) and 3.2082(5) (moiety I) intramolecular 3.1376(5) and 3.1653(5) (moiety II)

benzene ring C8–C13) with a C[⋯]Cg1 distance of 3.468(5) Å (Table S2). However, the hydrogen bonding net formed is complicated by the presence of a higher number of solvent molecules.

The water molecule with O28 acts as a bifurcated hydrogen-bond acceptor of the amine N–H from two distinct ligands and a hydrogen-bond donor in interactions with counterions, whereas the remaining water molecule (O29) interacts as a hydrogen-bond acceptor of one of the amine N–H groups and as a donor to counterions (Table S2, Figure 5).

Figure 5. Representation of the packing for **2b** viewed down the *b* axis; argentophilic interactions are shown as dashed grey lines, hydrogen bonds that involve water molecules are shown as red lines.

Crystal Structure of **3** Formed with CF₃SO₃[–] (Bulk Material **3**)

[AgL]CF₃SO₃·H₂O (**3a**)

Complex **3a** crystallises in the triclinic space group *P* $\bar{1}$ with unit cell parameters that are very similar to those observed for **2a**. Likewise, the packing is very similar to that of **2a** (Figure 4). The presence of water molecules and an elongated counterion in the crystal lattice influences the length of the *a* axis, which is ca. 0.75 Å longer than that in **2a**. The *b* axis, however, is slightly shorter, which could be caused by a small difference in the ligand conformation (see Table 3). Interactions between water molecules, triflate and the silver(I) complex further stabilise the packing (see Table S2).

Crystal Structures of **4a** and **4b** Formed with BF₄[–] (Bulk Material **4**)

{[AgL]BF₄}_n (**4a**)

Complex **4a** crystallises in the triclinic space group *P* $\bar{1}$. The cationic Ag^I complex forms 1D zigzag chains along the *a* axis, with the silver ions coordinated in a linear fashion by imine N atoms that originate from two distinct ligands (bridging mode, Figure 6). The conformation of the ligand facilitates this type of assembly (see Table 3).

Figure 6. Fragment of the cationic chain in **4a**; H atoms are omitted for clarity; displacement ellipsoids drawn at the 50% probability level. Selected bond lengths [Å] and angles [°]: Ag1–N1 2.093(8), Ag1–N17ⁱ 2.065(7), N17–Ag1–N1ⁱ 175.5(3). Symmetry operation: ⁱ: *x* + 1, *y*, *z*.

The bond lengths in the cationic unit are more or less in agreement with the distances observed for similar compounds (vide supra) with a C2–S6 distance of 1.727(9) Å in its shortest range [shorter bonds were reported for a Cd^{II} complex with deprotonated 4-(2-benzimidazolethiomethyl)-benzoic acid]^[11] and a long C16–N17 distance of 1.369(11) Å (for 22 bond lengths of a similar kind found in the crystal structure database, the mean is 1.324 Å).

The chains formed interact by argentophilic interactions with neighbouring chains to result in infinite strands supported by π – π interactions between corresponding imidazole rings (N1–C5) and (C16–N20) with a centroid–centroid distance of 3.722(6) Å and symmetry operation $-x, 2-y, 1-z$. Weak C–H[⋯]F and N–H[⋯]F hydrogen bonds between the cationic part and counterions stabilise the packing (see Table S2).

$[AgL]BF_4 \cdot xCH_3OH \cdot xH_2O$ (**4b**)

The quality of the crystals of **4b** was not sufficient to fully characterise the structure (see Table S1). The compound crystallises in the monoclinic space group $P2_1/c$ with unit cell parameters very similar to those obtained for **1a/1b**. The a and c axes are ca. 0.15 and 0.5 Å, respectively, which are shorter than those of the corresponding solvate **1b** and is attributed to the smaller size of the BF_4^- counterion.

Crystal Structures of 5a, 5b and 5c Formed with NO_3^- (Bulk Material 5)

$[Ag_2L(NO_3)_2]$ (**5a**)

Complex **5a** crystallises in the centrosymmetric space group $P\bar{1}$ (triclinic system). It has a 2:1 Ag/L molar ratio even though it was isolated from bulk material prepared with a molar ratio of 1:1. The resulting structure is unique as **L** shows bischelating behaviour (Figure 7). Ag1 is coordinated by imine N atoms to yield a linear geometry around the metal centre, which is distorted from linearity by interactions with nitrate counterions, namely, O24 [Ag–O 2.710(5) Å] and O23 [Ag–O 2.682(5) Å], which come from a symmetry related counterion (symmetry operation: $1 - x, -y, -z$). Defining the above mentioned O atoms with an Ag–O distance of ca. 2.7 Å as bonded, the complex could be described as a dimer with a seesaw geometry around Ag1 and a τ_4 value of 0.59.^[12] Ag2 is chelated by S-donor atoms that participate in its distorted tetrahedral environment (AgS_2O_2), whereby O atoms (O21 and O25) originate from two distinct nitrate counterions ($\tau_4 = 0.71$). Very strong intramolecular argentophilic interactions are present between the two metal centres, with a distance of ca. 2.96 Å, which is only slightly longer than that for metallic silver (2.89 Å).^[13]

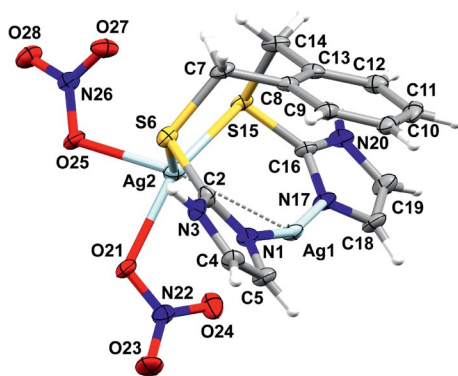


Figure 7. Molecular structure of **5a** with displacement ellipsoids drawn at the 50% probability level; argentophilic interactions are shown as dashed grey lines. Selected bond lengths [Å] and angles [°]: Ag1–N1 2.152(4), Ag1–N17 2.161(4), N17–Ag1–N1 163.56(16), Ag2–O21 2.334(4), Ag2–O25 2.417(4), Ag2–S6 2.539(1), Ag2–S15 2.475(1), O21–Ag2–O25 83.29(12), O21–Ag2–S15 146.52(9), O25–Ag2–S15 98.72(9), O21–Ag2–S6 98.42(10), O25–Ag2–S6 102.93(9), S15–Ag2–S6 113.41(4).

Not taking into account Ag2, the resulting packing (looking down the b axis) is reminiscent of that of **2a** and **3a**. However, intermolecular argentophilic interactions be-

tween neighbouring Ag1 atoms (distance ca. 4.46 Å) are not observed, which is due to the presence of the second silver centre, Ag2. For the same reason, there are no π – π interactions between imidazole rings from neighbouring units. In addition, the unit cell parameters are comparable with those of **2a** and **3a** with a shorter a axis, which is a result of much smaller counterions, and a longer c axis because of an additional silver atom.

The packing is stabilised by weak C10–H10 \cdots Cg3^{#3} hydrogen bonds [where Cg3 is the centroid of C16–N20, C10 \cdots Cg3 3.558(6) Å], as well as by many other weak C–H \cdots O and N–H \cdots O hydrogen bonding interactions (see Table S2).

$[AgL]NO_3 \cdot xH_2O$ (**5b**)

Complex **5b** crystallises in the centrosymmetric space group $P\bar{1}$ (triclinic system) with two cationic mononuclear metal complexes and two nitrate counterions in the asymmetric unit. The conformation of the ligand differs only slightly in the two cationic complexes. The silver ions are linearly coordinated by imine N atoms that originate from the chelating ligands (Figure 8), and the ligands adopt a folded conformation.

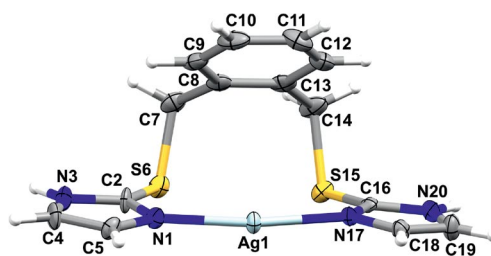


Figure 8. Representation of the cationic complex in **5a** with displacement ellipsoids drawn at the 50% probability level.

There is a noticeable distortion of AgN_2 from linearity (see Table 2), which could be caused by weak interactions with the nitrate O atoms [O23/O22A and O23A that are in the proximity (ca. 3.1 Å) of Ag1/Ag1A, respectively]. Looking down the a axis, columns of cationic complexes that consist exclusively of Ag1 or Ag1A units stacked above each other can be seen. The distance between the nearest Ag1 and Ag1A in those columns is 4.1084(6) Å, which shows the lack of interactions between these metal centres.^[10] Instead, the small nitrate counterions, which are located between the C1–N5/C1A–N5A imidazole rings of the stacked cationic units, form hydrogen bonds with the NH group of these as well as with the NH group from C16–N20/C16A–N20A of the adjacent columns. There are no π – π interactions present in the packing, which is stabilised by weak C–H \cdots S and C–H \cdots O interactions (Table S2). As the solvent molecules could not be modelled, and the final model was refined without them (by applying the SQUEEZE routine of PLATON), full analysis of the resulting packing was impossible.

$[Ag_3L_2NO_3][Ag_3L_2H_2O](NO_3)_5 \cdot 4H_2O$ (**5c**)

Complex **5c** crystallises in the centrosymmetric space group $P\bar{1}$ (triclinic system) and, just as **5a**, it shows an Ag/L

molar ratio of 1.5:1, even though it originated from bulk material prepared with a molar ratio of 1:1. Interestingly, there are two crystallographically independent cationic trinuclear moieties present in the asymmetric unit, as well as five nitrate counterions and four water molecules. Each cationic unit involves two folded **L** molecules with torsion angles C8–C7–S6–C2 –50.7(5)°, C13–C14–S15–C16 48.4(5)°, C28–C27–S26–C22 –45.0(4)°, C33–C34–S35–C36 55.5(4)°, C48–C47–S46–C42 50.3(4)°, C53–C54–S55–C56 –53.4(4)°, C68–C67–S66–C65 52.9(4)°, C73–C74–S75–C78 –53.9(4)°. The ligands show bischelating (*N,N*- and *S,S*-) behaviour as observed in **5a**. Furthermore, in each moiety there are three different geometries around the metal centres present in the structure. Namely, a linear geometry (AgN₂) is formed by one *N,N*-chelating ligand, a distorted tetrahedral environment (AgS₄) is formed by two *S,S*-chelating ligands and a T-shaped (AgN₂O) geometry is built up by the second *N,N*-chelating ligand and, surprisingly, by the counterion in one of the cationic moieties (moiety I) and the water molecule in the other one (moiety II, Figure 9). As a result, these two cationic units have different charges. They interact by hydrogen bonds such as N80–H80···O88, which involve the amine N atom from one of the imidazole rings of moiety II and the O atom from the coordinated nitrate anion (N86), and O81–H81B···O89^{#1} (for symmetry operation, see Table S2), which involve both

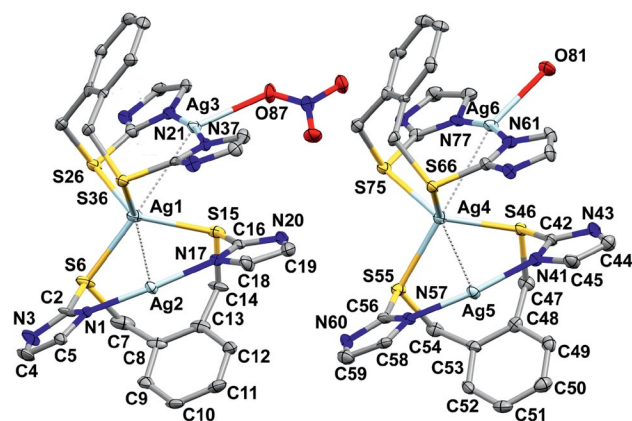


Figure 9. Representation of the two trinuclear cationic moieties with different O-donor ligands coordinated at one of the silver centres present in the asymmetric unit of **5c**. Hydrogen atoms and some labels are omitted for clarity; displacement ellipsoids drawn at the 50% probability level; intramolecular argentophilic interactions are shown as dashed grey lines. Selected bond lengths [Å] and angles [°]: (moiety I) Ag1–S15 2.538(1), Ag1–S35 2.558(1), Ag1–S6 2.603(1), Ag1–S26 2.604(1), N1–Ag2 2.115(4), Ag2–N 17 2.120(4), Ag3–N21 2.120(4), Ag3–N37 2.121(4), Ag3–O87 2.642(3), S15–Ag1–S35 112.77(4), S15–Ag1–S6 110.23(5), S35–Ag1–S6 120.64(5), S15–Ag1–S26 115.85(5), S35–Ag1–S26 106.98(4), S6–Ag1–S26 88.27(4), N1–Ag2–N17 168.35(16), N21–Ag3–N37 167.82(15), O87–Ag3–N21 85.19(13), O87–Ag3–N37 106.91(13); (moiety II) Ag4–S46 2.547(1), Ag4–S66 2.548(1), Ag4–S75 2.619(1), Ag4–S55 2.623(1), Ag5–N57 2.103(4), Ag5–N41 2.121(4), Ag6–N61 2.137(4), Ag6–N77 2.141(4), Ag6–O81 2.467(3), S46–Ag4–S66 113.02(4), S46–Ag4–S75 122.81(4), S66–Ag4–S75 102.82(4), S46–Ag4–S55 104.63(4), S66–Ag4–S55 123.51(4), S75–Ag4–S55 89.40(4), N57–Ag5–N41 169.19(15), N61–Ag6–N77 164.56(15), N61–Ag6–O81 102.26(14), N77–Ag6–O81 93.11(14).

coordinated O-donor ligands to form four-membered units. These are further interlinked by the counterion (N82) with hydrogen bonds O81–H81A···O85 and N23–H23···O83^{#5} into a 1D chain that expands along the *b* axis (Figure 10).

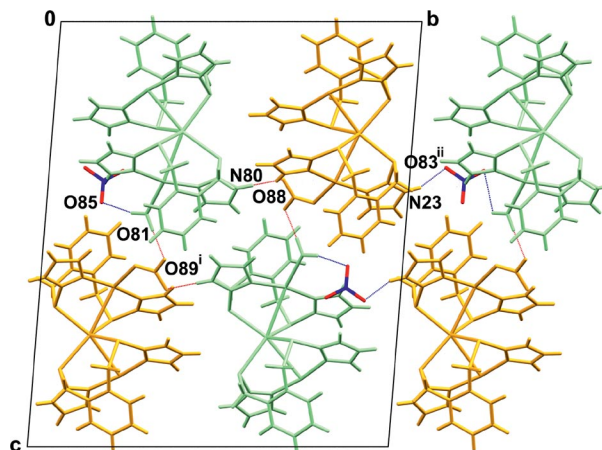


Figure 10. Fragment of the hydrogen bonded 1D chain in **5c** that consists of moieties I (orange) and II (green) shown in capped sticks representation. Symmetry operations: ^{#1}: $-x + 1, -y + 1, -z + 1$; ^{#5}: $x, y + 1, z$.

There are weak interactions present between Ag2 and O91/O91A and O93/O93A from the disordered nitrate counterion (N90) with distances of 2.70(2)–2.96(2) Å and between Ag5 and O103, O104 from another counterion (N102) with distances of 2.896(4) and 2.722(4) Å, respectively. The counterions N90 and N94 form hydrogen bonds with water molecule O115, which acts as a donor in this case but it is also a bifurcated hydrogen-bond acceptor for amine hydrogen atoms (H20–N20 and H40–N40). The counterions, N98 and N102 and three water molecules, such as O106, O109 and O112, form hydrogen bonded chains, which run along the *a* axis and interact by N–H···O with chains of cationic moieties to result in a 3D assembly. There are also other weak hydrogen bonds that support the packing (Table S2).

It seems that only one of the amine N atoms (N60) is not involved in the net of hydrogen bonds. A methanol molecule might have been present in the neighbourhood, which was lost as the crystals dried, to cause disorder of the N90 nitrate counterion and also yield the small solvent accessible voids nearby in the crystal lattice (PLATON estimates the accessible space to be 2.4% of the total cell volume).^[14]

Intramolecular argentophilic interactions (Table 4) and π – π interactions between imidazole rings (C16–N20 and C37–N40, N41–C45 and N61–C65) with centroid–centroid distances of ca. 3.4 Å are present in both trinuclear units.

Conclusions

This paper tackles the problem of the characterisation of the composition of bulk crystalline material. The presence of mixtures can be easily overlooked by C, H, N elemental analyses. It is still common practice among researchers to select one crystal from the final crystalline material and to

present this specimen as representative for the entire solid fraction. There is no requirement in journals to provide powder patterns as a proof of phase purity for solid samples.^[15] Therefore, the results can actually be very misleading and one might wonder how many papers describe elaborate solid-state studies performed on a mixture of metal–organic complexes. This is especially a risk in instances where research is conducted on extended, flexible (often multidonor) ligands and/or ligands that contain functional groups or atoms that have a tendency to form hydrogen bonds. In the latter case, the presence of solvates, and the replacement of the crystallisation solvent molecules with water upon exposure to air, seem to be very likely.^[16] The coordinating abilities of the counterions complicate matters even further.

1,2-Bis(imidazol-2-yl)thiomethylbenzene (**L**) is a good example of a ligand that is difficult to work with due to the heterogeneity of the crystalline material obtained. The amine nitrogen atoms increase the affinity to form different solvates through hydrogen bonding, which is not the case for imidazole-based linkers without an available amine N atom. The presence of additional S-donor atoms makes any structural prediction even more complicated. The ligand generally shows a tendency to form discrete *N,N*-bidentate mononuclear Ag^I complexes with a linear geometry around the metal centre, induced by the chelating imine nitrogen atoms of the folded ligand, with the imidazole rings approximately coplanar. However, other modes of coordination can also take place, such as *N,N'*-bridging, participation of S-donor atoms or a T-shaped geometry around the silver atom, brought about by the chelating N atoms of the ligand in combination with solvent molecules or counterions.

Further studies that aim to control both the conformation of the ligand and the coordination modes, which involve exocyclic S-donor sites as in **5a** and **5c**, are ongoing.

Experimental Section

Reagents: All commercially available chemicals were of reagent grade and were used without further purification. 1,2-Bis(imidazol-2-yl)thiomethylbenzene (**L**) was synthesised by the S_N2 reaction of 2-mercaptoimidazole with *α,α'*-dibromo-*o*-xylol in MeOH. ¹H NMR (300 MHz, [D₆]DMSO): δ = 12.16 (br. s, 2 H), 7.15 (m 4 H), 7.06 (s, 4 H), 4.34 (s, 4 H) ppm. ¹³C NMR (100 MHz, [D₆]DMSO): δ = 138.1, 135.9, 130.1, 127.6, 35.2 ppm. C₁₄H₁₄N₄S₂ (302.41): calcd. C 55.60, H 4.67, N 18.53; found C 55.49, H 4.89, N 18.61.

Crystalline Bulk Materials: Compound **1** was obtained by the reaction of AgPF₆ with **L**. From this batch, four different crystal structures were determined: [AgL]PF₆·CH₃OH (**1a**), [AgL]PF₆·H₂O (**1b**), [AgL]PF₆·*x*CH₃OH·*x*H₂O (**1c**) and [AgLCH₃O(H)_{0.5}](PF₆)_{0.5} (**1d**). Compound **2** was obtained by the reaction of AgSbF₆ with **L**. From this batch, two different crystal structures were determined: [AgL]SbF₆ (**2a**) and [AgL]SbF₆·1.5H₂O (**2b**). Compound **3** was obtained by the reaction of AgCF₃SO₃ with **L**. From this batch, one crystal structure was determined: [AgL]CF₃SO₃·H₂O (**3a**). Compound **4** was obtained by the reaction of AgBF₄ with **L**. From this batch, two crystal structures were determined: {[AgL]BF₄}_{*n*} (**4a**) and [AgL]BF₄·*x*CH₃OH·*x*H₂O (**4b**). Compound **5** was obtained by the reaction of AgNO₃ with **L**. From this batch, three

crystal structures were determined: [Ag₂L(NO₃)₂] (**5a**), [AgL]NO₃·*x*H₂O (**5b**) and [Ag₃L₂NO₃][Ag₃L₂H₂O](NO₃)₅·4H₂O (**5c**). The water in the crystals can be attributed to the presence of water in the methanol and/or to air moisture, as the crystals were grown by slow evaporation in ambient air (methanol in the crystal lattice was replaced by water over time, as was noted before by the author for similar systems).

Structure Determination: Single-crystal X-ray diffraction data were collected with a Bruker SMART APEX diffractometer equipped with graphite monochromated Mo-*K*_α radiation (λ = 0.71073 Å).^[17a] The crystals were mounted on a glass fibre and coated with Paratone-N oil. Data collection was carried out at 100(2) K to minimise solvent loss, possible structural disorder and thermal motion effects. Cell refinement and data reduction were performed using the program SAINT^[17b] and all empirical absorption corrections were performed using SADABS.^[17c] Each structure was solved by direct methods using SHELXS-97 and refined by full-matrix least-squares methods based on *F*² using SHELXL-97.^[17d] The program Mercury was used to prepare molecular graphics images.^[17e] Hydrogen atoms, excluding those from OH (water, methanol) were positioned geometrically with C–H 0.95 (aromatic), 0.98 (methyl) and 0.99 Å (methylene); N–H 0.88 Å (aromatic) and refined as riding, with *U*_{iso}(H) = 1.2 *U*_{eq}(C, N) and 1.5 *U*_{eq}(methyl C). The remainder were located in a difference map and refined with restrained O–H bond lengths. Data collection and structure refinement parameters are presented in Table 1. Crystal structures **1a**, **1d**, **2a**, **2b**, **3a**, **5a** and **5c** were deposited with the CCDC. The remaining crystal structures **1b**, **1c**, **4a**, **4b** and **5b** are described briefly in the text (poor data quality for **1c** and **4b** does not allow for in depth discussion). In **1b**, the water molecule was disordered and modelled in four positions. In **4a**, the anisotropic displacement parameters were restrained for C8, C9, C10 and N17. In **5b**, the electron density was subtracted and the SQUEEZE instruction of PLATON was applied^[17f] as it was impossible to find a suitable refinement model because of highly disordered water molecules. From this calculation we can estimate the presence of two water molecules in the asymmetric unit. However, in the tabulated data (Table 1) the molecular formula and weight, *F*(0 0 0) and absorption coefficient were not corrected for the presence of solvent molecules. In this crystal structure, the anisotropic displacement parameters were restrained for O43 and O48. In **5c** one of the counterions (N90) is disordered over two positions with refined site occupancies of 0.65(2):0.35(2). As a result, geometrical and displacement-parameter restraints were applied to this anion.

CCDC-839088 (for **1a**), -839089 (for **1d**), -839090 (for **2a**), -839091 (for **2b**), -839092 (for **3a**), -839093 (for **5a**) and -839094 (for **5c**) contain the supplementary crystallographic data for this paper. These data can be obtained free of charge from The Cambridge Crystallographic Data Centre via www.ccdc.cam.ac.uk/data_request/cif.

Supporting Information (see footnote on the first page of this article): Crystal data and details of the refinement parameters for the crystal structures originating from crystalline bulk material **1–5** (Table S1). Parameters for hydrogen bonding in **1–5** (Table S2) as well as figures presenting XRPD patterns for solids **1–5** (experimental and calculated for isolated phases).

Acknowledgments

The author thanks the Research Foundation Flanders (FWO) for financial support and the National Research Foundation (NRF) of South Africa for supporting this work in its initial stage. Special

thanks are directed to Prof. Wim Dehaen and Dr Jo Alen for support during the writing process.

- [1] a) M. B. Duriska, S. M. Neville, S. R. Batten, *Chem. Commun.* **2009**, 5579–5581; b) D. Kim, J. H. Paek, M.-J. Jun, J. Y. Lee, S. O. Kang, J. Ko, *Inorg. Chem.* **2005**, *44*, 7886–7894; c) L. Carlucci, G. Ciani, D. M. Proserpio, *Coord. Chem. Rev.* **2003**, *246*, 247–289; d) G. F. Swiegers, T. J. Malefetse, *Chem. Rev.* **2000**, *100*, 3483–3537.
- [2] a) G. Férey, C. Serre, T. Devic, G. Maurin, H. Jobic, P. L. Llewellyn, G. De Weireld, A. Vimont, M. Daturif, J.-S. Chang, *Chem. Soc. Rev.* **2011**, *40*, 550–562; b) M. Clemente-León, E. Coronado, C. Martí-Gastaldo, F. M. Romero, *Chem. Soc. Rev.* **2011**, *40*, 473–497; c) C. Janiak, J. K. Vieth, *New J. Chem.* **2010**, *34*, 2366–2388.
- [3] a) C. A. Matuszak, A. J. Matuszak, *J. Chem. Educ.* **1976**, *53*, 280–284; b) M. L. Goodgame, M. Goodgame, P. J. Hayward, G. W. Rayner-Canham, *Inorg. Chem.* **1968**, *7*, 2447–2451; c) J. E. Bauman, J. Wang, *Inorg. Chem.* **1964**, *3*, 368–373.
- [4] a) S.-L. Li, Y.-Q. Lan, J.-C. Ma, J.-F. Ma, Z.-M. Su, *Cryst. Growth Des.* **2010**, *10*, 1161–1170; b) H.-Y. Bai, J.-F. Ma, J. Yang, Y.-Y. Liu, H. Wu, J.-C. Ma, *Cryst. Growth Des.* **2010**, *10*, 995–1016; c) L.-P. Zhang, J.-F. Ma, J. Yang, Y.-Y. Liu, G.-H. Wei, *Cryst. Growth Des.* **2009**, *9*, 4660–4673; d) L. Carlucci, G. Ciani, S. Maggini, D. M. Proserpio, *CrystEngComm* **2008**, *10*, 1191–1203.
- [5] a) L. Dobrzańska, *CrystEngComm* **2011**, *13*, 2303–2309; b) L. Dobrzańska, D. J. Kleinhans, L. J. Barbour, *New J. Chem.* **2008**, *32*, 813–819; c) L. Dobrzańska, G. O. Lloyd, C. Esterhuyzen, L. J. Barbour, *Angew. Chem.* **2006**, *118*, 5988; *Angew. Chem. Int. Ed.* **2006**, *45*, 5856–5859.
- [6] Recently, a paper on the treatment of Cd^{II} complexes with 1,3-bis([imidazol-2-yl]thiomethyl)-2,4,6-trimethylbenzene was published. One of the authors was a student working under the supervision of the author of this article (S. V. Potts, L. J. Barbour, *New J. Chem.* **2010**, *34*, 2451–2457). Somehow the name of the senior author was not included in the publication. The nomenclature of the ligand is not correct in this article, where it features as “1,3-bis(1-imidazolyl-2-thione)-2,4,6-trimethylbenzene”.
- [7] For structural studies on metal complexes with extended ligands that contain a benzene core and thioether functionality see: **aniline-based**: a) Ag^I: Y. Zheng, S.-L. Wang, *Acta Crystallogr., Sect. C* **2004**, *60*, m278–m279; **benzene-based**: b) Ag^I: X.-H. Bu, W.-F. Hou, M. Du, W. Chen, R.-H. Zhang, *Cryst. Growth Des.* **2002**, *2*, 303–307. **benzimidazole-based**: c) Ag^I: C. Fan, C. Ma, C. Chen, F. Chen, Q. Liu, *Inorg. Chem. Commun.* **2003**, *6*, 491–494; **imidazole-based**: d) Cd^{II}, Zn^{II}: J. K. Voo, C. D. Incavito, G. P. A. Yap, A. L. Rheingold, C. G. Riordan, *Polyhedron* **2004**, *23*, 405–412; e) Cu^I J. K. Voo, K. C. Lam, A. L. Rheingold, C. G. Riordan, *J. Chem. Soc., Dalton Trans.* **2001**, 1803–1805; **pyridine-based**: f) Cu^{II}: D. A. McMorran, C. M. Hartshorn, P. J. Steel, *Polyhedron* **2004**, *23*, 1055–1061; g) Co^{II}: Z. Atherton, D. M. L. Goodgame, S. Menzer, D. J. Williams, *Polyhedron* **1999**, *18*, 273–279; h) Ag^I: C. M. Hartsorn, P. J. Steel, *J. Chem. Soc., Dalton Trans.* **1998**, 3935–3940; **pyrimidine-based**: i) Cu^{II}: R. Peng, S.-H. Lin, Y.-Y. Yang, *Acta Crystallogr., Sect. E* **2007**, *63*, m2385; j) Cu^I R. Peng, D. Li, T. Wu, X.-P. Zhou, S. W. Ng, *Inorg. Chem.* **2006**, *45*, 4035–4046; k) Cu^I: R. Peng, T. Wu, D. Li, *CrystEngComm* **2005**, *7*, 595–598; l) Ag^I: L. Han, B. Wu, Y. Xu, M. Wu, Y. Gong, B. Lou, B. Chen, M. Hong, *Inorg. Chim. Acta* **2005**, *358*, 2005–2013; m) Ag^I: R.-H. Wang, M.-C. Hong, W.-P. Su, Y.-C. Liang, R. Cao, Y.-J. Zhao, J.-B. Weng, *Polyhedron* **2001**, *20*, 3165–3170; n) Ag^I: M. Hong, W. Su, R. Cao, M. Fujita, J. Lu, *Chem. Eur. J.* **2000**, *6*, 427–431; **pyridyl-pyrimidine-based**: o) Cd^{II}, Zn^{II}: H. Dong, H. Zhu, T. Tong, S. Gou, *J. Mol. Struct.* **2008**, *891*, 266–271; p) Ag^I, Hg^{II}: H.-Z. Dong, H.-B. Zhu, X. Liu, S.-H. Gou, *Polyhedron* **2008**, *27*, 2167–2174; **thiadiazole-based**: q) Ag^I: Y. Zheng, *Acta Crystallogr., Sect. C* **2004**, *60*, m471–m472; **quinoline-based**: r) Cu^I, Cu^{II}: C.-Y. Su, S. Liao, M. Wanner, J. Fiedler, C. Zhang, B.-S. Kang, W. Kaim, *Dalton Trans.* **2003**, 189–202; s) Cu^I, Cu^{II}: S. Tavecchi, T. A. Miller, R. L. Paul, J. C. Jeffery, M. D. Ward, *Polyhedron* **2003**, *22*, 507–514; t) Ag^I: S. Liao, C.-Y. Su, H.-X. Zhang, J.-L. Shi, Z.-Y. Zhou, H.-Q. Liu, A. S. C. Chan, B.-S. Kang, *Inorg. Chim. Acta* **2002**, *336*, 151–156.
- [8] L. Dobrzańska, E. J. C. de Vries, *Inorg. Chim. Acta* **2007**, *360*, 1584–1592.
- [9] a) XRPD intensities for **1–5** were measured with a Bruker D8 Advance Diffractometer (Cu-K_α, λ = 1.54056 Å) at ambient temperature; b) W. Kraus, G. Nolze, *PowderCell 2.4*, Federal Institute for Materials Research and Testing, Berlin, Germany, **1999**; c) *PowderCell*, v. 2.4 was used for Rietveld refinement (mass-%): the background was approximated with 8th order polynomials; diffraction lines were fitted to pseudo-Voigt profile function; for **1c** assuming the presence of 1.5 H₂O molecules per molecular formula; for **4b** assuming the presence of one MeOH molecule per molecular formula; for **5b** assuming the presence of one H₂O molecule per molecular formula (estimates based on *SQUEEZE*). Due to the assumptions made above and uncertainty whether all crystallographic phases have been identified, the results should be considered “tentative”.
- [10] The majority of the papers refer to a value of 3.44 Å for a cut off for argentophilic interactions, which is twice the van der Waals radius based on a paper by Bondi (a) A. Bondi, *J. Phys. Chem.* **1964**, *68*, 441–451) but he clearly states that the van der Waals values of metallic elements have a purely tentative nature. For more recent values of van der Waals radii (2.05/2.1 Å) see: b) S. S. Batsanov, *J. Mol. Struct.* **2011**, *990*, 63–66; c) S. Nag, K. Banerjee, D. Datta, *New J. Chem.* **2007**, *31*, 832–834; d) S. S. Batsanov, *Inorg. Mater.* **2001**, *37*, 871–885.
- [11] L. Han, Y. Gong, D. Yuan, M. Hong, *J. Mol. Struct.* **2006**, *789*, 128–132.
- [12] For a discussion of Ag–L cut-off values, see: A. G. Young, L. R. Hanton, *Coord. Chem. Rev.* **2008**, *252*, 1346–1386; for geometry index τ₄ (defined as “the sum of angles α and β – the two largest θ angles in the four-coordinate species – subtracted from 360°, all divided by 141°”), see: L. Yang, D. R. Powell, R. P. Houser, *Dalton Trans.* **2007**, 955–964.
- [13] a) B. Cordero, V. Gómez, A. E. Platero-Prats, M. Revés, J. Echeverría, E. Cremades, F. Barragán, S. Alvarez, *Dalton Trans.* **2008**, 2832–2838; b) L. Pauling, *The Nature of the Chemical Bond*, 3rd ed., Cornell University Press, Ithaca, NY, **1980**, p. 403.
- [14] A. L. Spek, *PLATON*, A Multipurpose Crystallographic Tool, Utrecht University, Utrecht, The Netherlands, **2001**.
- [15] It is surprising that in many cases, even though the authors provide powder patterns (experimental and generated from the crystal structures) as proof of phase purity, they differ enough to assume the presence of mixtures.
- [16] a) L. F. Jones, K. D. Camm, C. A. Kilner, M. A. Halcrow, *CrystEngComm* **2006**, *8*, 719–728; b) C.-Y. Su, B.-S. Kang, C.-X. Du, Q.-C. Yang, T. C. W. Mak, *Inorg. Chem.* **2000**, *39*, 4843–4849.
- [17] a) *SMART*, version 5.625, Bruker AXS Inc., Madison, Wisconsin, USA, **2001**; b) *SAINT*, version 6.36a, Bruker AXS Inc., Madison, Wisconsin, USA, **2002**; c) G. M. Sheldrick, *SADABS*, version 2.05, University of Göttingen, Germany, **1997**; d) G. M. Sheldrick, *Acta Crystallogr., Sect. A* **2008**, *64*, 112–122; e) C. F. Macrae, I. J. Bruno, J. A. Chisholm, P. R. Edgington, P. McCabe, E. Pidcock, L. Rodriguez-Monge, R. Taylor, J. van de Streek, P. A. Wood, *J. Appl. Crystallogr.* **2008**, *41*, 466–470; f) *PLATON/SQUEEZE*: P. van der Sluis, A. L. Spek, *Acta Crystallogr., Sect. A* **1990**, *46*, 194–201.

Received: August 16, 2011

Published Online: January 23, 2012